J. D. Silva
jornandes.dias@pq.cnpq.br
Tel: (081) 3184-7529
University of Pernambuco – UPE
Polytechnic School in Recife
Environmental and Energetic Tech. Laboratory
Rua Benfica, 455, Madalena
50750-470 Recife, PE, Brazil

Dynamic Evaluation for Liquid Tracer in a Trickle Bed Reactor

A mathematical model is developed for a liquid flow on solid particles in a trickle bed reactor. A mathematical formulation is followed based on the liquid-solid model approach where the liquid phase with the (KCl) tracer is treated as a continuum. The physical modeling is discussed, including the formulation of initial and boundary conditions and the description of the solution methodology. Results of mathematical model are presented and validated. The model is validated through comparison using three experimental cases. The optimized values of the axial dispersion (D_{ax}), liquid-solid mass transfer (k_{LS}), and partial wetting efficiency (F_M) coefficients are obtained simultaneously using the objective function. The behavior of D_{ax}, k_{LS}, and F_M is analyzed by the empirical correlations.
Keywords: *liquid-solid model, mathematical modeling, experimental, liquid tracer, TBRs*

Introduction

Gas-liquid-solid reactors with the packed bed of solid particles can be operated in three forms, depending upon the orientation of gas-liquid flows. Gas-liquid flows can be concurrently downflows, cocurrently upflows, and downflow of liquid and countercurrent upflow of gas. The reactor in which gas-liquid flows concurrently downflow is conventionally referred to as a trickle bed reactor (Satterfield et al., 1978). The purpose of this work is associated with trickle bed reactors (TBRs). TBRs are very competitive both technologically and economically because they offer many advantages, such as high conversion, small liquid-solid ratio, small resistance to the diffusion of gaseous reactant to the solid surface, and low pressure drop.

TBRs are widely used in industrial applications. The largest applications of TBRs occur in industrial processes, including hydrotreating, hydrodesulfurization, petroleum refining, petrochemical, hydrogenation, oxidation, hydrodenitrogenation, biochemical, and detoxification of waste water industries (Al-Dahhan et al., 1997; Dudukovic et al., 1999; Liu et al., 2008; Ayude et. al., 2008; Augier et al., 2010; Rodrigo et al., 2009).

Mathematical models of TBRs represent an important tool for minimizing the experimental efforts required for developing this equipment in industrial plants. Mathematical modeling and numerical simulation of TBR_S are in continuous development, contributing in a increasing form for the better understanding of processes and physical phenomena of TBRs. Mathematical models have to be validated with experimental data and these experimental data involve complex measurements of difficult accomplishment.

Mathematical modeling of TBRs may involve the mechanisms of forced convection, axial dispersion, interphase mass transport, intraparticle diffusion, adsorption, and chemical reaction. Normally, these models are constructed relating each phase to the others (Silva et al., 2003; Burghardt et al., 1995; Iliuta et al., 2002; Latifi et al., 1997).

The objective of the work is to estimate and describe the behavior of the axial dispersion (D_{ax}), liquid-solid mass transfer (k_{LS}), and partial wetting efficiency (F_M) coefficients using a set of experiments carried out in a laboratory scale TBR. By comparison the theoretical model is validated using experimental cases.

Nomenclature

$A_L(z,t)$ = *concentration of the liquid tracer in the liquid phase, kg* m^{-3}
$A_S(z,t)$ = *concentration of the liquid tracer in the external surface of solid, kg* m^{-3}
a_{LS} = *effective liquid-solid mass transfer area per unit column volume,* $m^2\ m^{-3}$
D_{ax} = *axial dispersion coefficient for the liquid tracer in the liquid phase,* $m^2\ s^{-1}$
D_L = *liquid molecular diffusivity,* $m^2\ s^{-1}$
d_P = *diameter of the catalyst particle, m*
d_r = *diameter of the reactor, m*
F = *objective function*
F_M = *wetting factor, dimensionless*
Ga_L = *Galileo number,* $\mathrm{Ga_L} = \mathrm{d_p^3\, g\, \rho_L^2 / \mu_L}$
$h_{d,L}$ = *dynamic liquid holdup, dimensionless*
i = *complex number* $\sqrt{-1}$
k_{LS} = *liquid-solid mass transfer coefficient, m* s^{-1}
k_r = *reaction constant, kgmol* $kg^{-1}\ s^{-1}$
L = *height of the catalyst bed, m*
$N_L(\xi)$ = *defined function in Eq. (16)*
P_E = *Peclet number,* $P_E = V_{SL}\, L / D_{ax}$
Re_L = *Reynolds number,* $Re_L = V_{SL}\, \rho_L\, d_r / \mu_L$
Re_G = *Reynolds number,* $Re_G = V_{SG}\, \rho_G\, d_r / \mu_G$
Sc_L = *Schmidt number,* $Sc_L = \mu_L / \rho_L\, D_L$
t = *time, s*
V_{SL} = *superficial velocity of the liquid phase, m* s^{-1}
z = *axial distance of the catalytic reactor, m*
$Z_L(t_d)$ = *function defined in Eq.* (16)

Greek Symbols

α_{LS} = *parameter defined in Eq.* (11), *dimensionless*
β_S = *parameter defined in Eq.* (13), *dimensionless*
ε_{ex} = *external porosity, dimensionless*
ε_P = *bed porosity, dimensionless*
$\Psi_i(\xi,t_d)$ = *dimensionless concentration of the tracer in liquid and solid, i = L, S*
η = *catalytic effectiveness factor*
μ_L = *viscosity of the liquid phase, kg* $m^{-1}\ s^{-1}$
ξ = *parameter defined in Table 1, dimensionless*
ρ_L = *density of the liquid phase, kg* m^{-3}

Mathematical Model

In this work, the modeling adopted is based on the liquid-solid model, which treats the liquid phase (H_2O + KCl tracer) as a continuum on a packed bed of solid particles. A one-dimensional mathematical model is adopted, in which the axial dispersion, liquid-solid mass transfer, partial wetting, and reaction phenomena are present. This model is used for the liquid phase using the KCl as tracer and it is restricted to the following assumptions: (i) isothermal system; (ii) all flow rates are constant throughout the reactor; (iii)

**Paper received 5 August 2010. Paper accepted 5 February 2011.
Technical Editor: Francisco Cunha**

the intraparticle diffusion resistance is neglected; (iv) in any position of the reactor the chemical reaction rate within the solid is equal to the liquid-solid mass transfer rate.

- Mass balance for the liquid:

$$h_{d,L}\frac{\partial A_L(z,t)}{\partial t}+V_{SL}\frac{\partial A_L(z,t)}{\partial z}=D_{ax,L}\frac{\partial^2 A_L(z,t)}{\partial z^2}-(1-\varepsilon_P)\,F_M\,k_{LS}a_{LS}[A_L(z,t)-A_S(z,t)] \quad (1)$$

- The initial and boundary conditions for Eq. (1) are:

$$A_L(z,0)=A_{L,0} \quad (2)$$

$$\left.\frac{\partial A_L(z,t)}{\partial z}\right|_{z=0^+}=\frac{V_{SL}}{D_{ax,L}}\left[A_L(z,t)|_{z=0+}-A_L(z,0)\right] \quad (3)$$

$$\left.\frac{\partial A_L(z,t)}{\partial z}\right|_{z=L}=0 \quad (4)$$

- Combining the chemical reaction rate with the mass transfer rate:

$$k_{LS}a_{LS}[A_L(z,t)-A_S(z,t)]=k_r\,A_S(z,t)\eta\varepsilon_P \quad (5)$$

Equations (1) to (5) can be analyzed with dimensionless variable terms, see Table (1):

Table 1. Summary of dimensionless variables.

dimensionless liquid concentration	$\psi_L(\xi,t_d)=\frac{A_L(z,t)}{A_{L,0}}$
dimensionless solid concentrations	$\psi_S(\xi,t_d)=\frac{A_S(z,t)}{A_{L,0}}$
dimensionless time	$t_d=\frac{V_{SL}\,t}{L\,h_{d,L}}$
dimensionless coordinate axial direction	$\xi=\frac{z}{L}$

Writing Eqs. (1) to (5) in dimensionless forms:

$$\frac{\partial\psi_L(\xi,t_d)}{\partial t_d}+\frac{\partial\psi_L(\xi,t_d)}{\partial\xi}=\frac{1}{P_E}\frac{\partial^2\psi_L(\xi,t_d)}{\partial\xi^2}-\alpha_{LS}[\psi_L(\xi,t_d)-\psi_S(\xi,t_d)] \quad (6)$$

$$\psi_L(\xi,0)=1 \quad (7)$$

$$\left.\frac{\partial\psi_L(\xi,t_d)}{\partial\xi}\right|_{\xi=0^+}=P_E\left[\psi_L(\xi,t_d)|_{\xi=0^+}-1\right] \quad (8)$$

$$\left.\frac{\partial\psi_L(\xi,t_d)}{\partial\xi}\right|_{\xi=1}=0 \quad (9)$$

$$\psi_L(\xi,t_d)-\psi_S(\xi,t_d)=\beta_S\,\psi_S(\xi,t_d) \quad (10)$$

Equations (6) through (10) include the following dimensionless parameters:

$$\alpha_{LS}=\frac{(1-\varepsilon_P)\,F_M\,k_{LS}\,a_{LS}\,L}{V_{SL}} \quad (11)$$

$$P_E=\frac{V_{SL}\,L}{D_{ax,L}} \quad (12)$$

$$\beta_S=\frac{k_r\,\eta\,\varepsilon_P}{k_{LS}\,a_{LS}} \quad (13)$$

Analytical Solution

The solution of transport problems in three-phase systems is very complex and usually numerical approximation methods are used. On the other hand, analytical solutions are used for the simple models. Although the analytical solutions are simple, the boundary conditions proposed for these models need a careful attention. The majority of the analytical solutions belong to infinite and semi-infinite field. The analytical solutions for the finite field have been developed by Feike and Torid (1998) and Dudukovic (1982). In this work, the author adopt the analytical procedure in the finite field region ($0 \le z \le L \rightarrow 0 \le \xi \le 1$) where the method of separation of variables is used.

The $\psi_S(\xi, t_d)$ was isolated from Eq. (10) and it was introduced in Eq. (6), reducing it to:

$$\frac{\partial\psi_L(\xi,t_d)}{\partial t_d}+\frac{\partial\psi_L(\xi,t_d)}{\partial\xi}=\frac{1}{P_E}\frac{\partial^2\psi_L(\xi,t_d)}{\partial\xi^2}-\gamma\,\psi_L(\xi,t_d) \quad (14)$$

where:

$$\gamma=\frac{\alpha_{LS}\,\beta_S}{\beta_S+1} \quad (15)$$

The analytical solution of Eq. (14) was obtained by the separation of variables method using the following relation:

$$\psi_L(\xi,t_d)=N_L(\xi)*Z_L(t_d) \quad (16)$$

Then, Eq. (14) was separated in two ordinary differential equations with constant coefficients:

$$\frac{dZ_L(t_d)}{dt_d}+\lambda^2 Z_L(t_d)=0 \quad (17)$$

$$\frac{d^2N_L(\xi)}{d\xi^2}-\frac{dN_L(\xi)}{d\xi}+\left(\lambda^2-\gamma\right)P_E\,N_L(\xi)=0 \quad (18)$$

The global solution of Eqs. (17) and (18) is given by:

$$\psi_L(\xi,t_d) = e^{-\lambda^2 t_d}\left\{\frac{1}{2}\left\{C_1 e^{\frac{i}{2}\left[4P_E\left(\lambda^2-\gamma\right)-1\right]^{1/2}\xi} + C_2 e^{-\frac{i}{2}\left[4P_E\left(\lambda^2-\gamma\right)-1\right]^{1/2}\xi}\right\}\xi\right\} \quad (19)$$

Transforming Eq. (19) in its trigonometric form:

$$e^{\frac{i}{2}\left[4P_E\left(\lambda^2-\gamma\right)-1\right]^{1/2}\xi} = \cos\frac{1}{2}\left[4P_E\left(\lambda^2-\gamma\right)-1\right]^{1/2}\xi + i\sin\frac{1}{2}\left[4P_E\left(\lambda^2-\gamma\right)-1\right]^{1/2}\xi \quad (20)$$

$$e^{-\frac{i}{2}\left[4P_E\left(\lambda^2-\gamma\right)-1\right]^{1/2}\xi} = \cos\frac{1}{2}\left[4P_E\left(\lambda^2-\gamma\right)-1\right]^{1/2}\xi - i\sin\frac{1}{2}\left[4P_E\left(\lambda^2-\gamma\right)-1\right]^{1/2}\xi \quad (21)$$

then:

$$\psi_L(\xi,t_d) = \left\{K_1 e^{\frac{1}{2}[\cos\varphi(\lambda)\xi]\xi} + K_2 e^{\frac{1}{2}[\sin\varphi(\lambda)\xi]\xi}\right\} e^{-\lambda^2 t_d} \quad (22)$$

where:

$$\varphi(\lambda) = \frac{1}{2}\left[4P_E\left(\lambda^2-\gamma\right)-1\right]^{1/2} \quad (23)$$

Applying $t_d \to \infty$ to the above equation and using the boundary conditions given by Eqs. (8) and (9), the eigenvalue expression was obtained:

$$\cot g\,\varphi(\lambda) = \frac{\left\{4\left[1-2P_E\left(\lambda^2-\gamma\right)\right]^2\left[4P_E\left(\lambda^2-\gamma\right)-1\right]\right\}^{1/2}}{8P_E^2\left(\lambda^2-\gamma\right)-P_E\left(\lambda^2-\gamma\right)+1} \quad (24)$$

Eq. (24) is a transcendental equation and it can be solved graphically. From this solution, the intermediary values for λ_n as: $\lambda_n = (2\,n + ½)$; (n = 0, 1, 2, 3, ...) were found, so that, the global solution for the concentration distribution in the reactor was obtained by Fourier series.

$$\psi_L(\xi,t_d) = \sum_{n=0}^{\infty}\left\{K_{1,n} e^{\frac{1}{2}[\cos\varphi_n(\lambda_n)\xi]\xi} + K_{2,n} e^{\frac{1}{2}[\sin\varphi_n(\lambda_n)\xi]\xi}\right\} e^{-\lambda_n^2 t_d} \quad (25)$$

where:

$$\varphi_n(\lambda_n) = \frac{1}{2}\left\{4P_E\left\{\left[\left(2n+\tfrac{1}{2}\right)\pi\right]^2-\gamma\right\}-1\right\}^{1/2} \quad (26)$$

$K_{1,n}$ and $K_{2,n}$ are the integral constants and they are obtained by orthogonality from the initial condition according to the following procedure: (a) Eq. (25) was multiplied by $\sin\varphi_n(\lambda_n)\xi$ and their initial condition was introduced; (b) Eq. (25) was then multiplied by $\cos\varphi_n(\lambda_n)\xi$ and their initial condition was applied; (c) the resulting equation of items a and b were integrated from 0 to 1, leading to:

$$K_{1,n}\,T_{1,n}(\lambda_n) + K_{2,n}\,T_{2,n}(\lambda_n) = 1-\cos\varphi_n(\lambda_n) \quad (27)$$

$$K_{1,n}\,T_{3,n}(\lambda_n) + K_{2,n}\,T_{4,n}(\lambda_n) = \sin\varphi_n(\lambda_n) \quad (28)$$

where the terms $T_{1,n}$, $T_{2,n}$, $T_{3,n}$ and $T_{4,n}$ are given by:

$$T_{1,n}(\lambda_n) = \frac{\{\varphi_n(\lambda_n)[3.2\sin\varphi_n(\lambda_n)\cos\varphi_n(\lambda_n)+0.6\varphi_n(\lambda_n)]}{1+16[\varphi_n(\lambda_n)]^2} + \sin^2\varphi_n(\lambda_n)\,[0.8+25.6[\varphi_n(\lambda_n)]^2\}\} \quad (29)$$

$$T_{2,n}(\lambda_n) = \frac{\varphi_n(\lambda_n)}{1+16[\varphi_n(\lambda_n)]^2}\left\{\begin{matrix}3.3\sin^2\varphi_n(\lambda_n)-13.2\sin\varphi_n(\lambda_n)\\ \cos\varphi_n(\lambda_n)+0.4[\varphi_n(\lambda_n)]\end{matrix}\right\} \quad (30)$$

$$T_{3,n}(\lambda_n) = \frac{\{3.3\,\varphi_n(\lambda_n)\cos^2\varphi_n(\lambda_n)+13.2\,[\varphi_n(\lambda_n)]^2+\cos\varphi_n(\lambda_n)}{1+16[\varphi_n(\lambda_n)]^2} \sin\varphi_n(\lambda_n)-2\,\varphi_n(\lambda_n)-10.4\,[\varphi_n(\lambda_n)]^3\} \quad (31)$$

$$T_{4,n}(\lambda_n) = \frac{\{1.6\sin^2\varphi_n(\lambda_n)\{1+16[\varphi_n(\lambda_n)]^2\}+3.2\,\varphi_n(\lambda_n)}{1+16[\varphi_n(\lambda_n)]^2} \cos\varphi_n(\lambda_n)\sin\varphi_n(\lambda_n)-10.4\,[\varphi_n(\lambda_n)]^3\}\} \quad (32)$$

In Equations (27) and (28), the constants $K_{1,n}$ and $K_{2,n}$ were obtained as:

$$K_{1,n} = \frac{\{T_{2,n}(\lambda_n)\sin\varphi_n(\lambda_n) - T_{4,n}(\lambda_n)[1-\cos\varphi_n(\lambda_n)]\}}{T_{2,n}(\lambda_n)\,T_{3,n}(\lambda_n) - T_{1,n}(\lambda_n)T_{4,n}(\lambda_n)} \quad (33)$$

$$K_{2,n} = \frac{\{T_{3,n}(\lambda_n)[1-\cos\varphi_n(\lambda_n)] - T_{1,n}(\lambda_n)\sin\varphi_n(\lambda_n)\}}{T_{2,n}(\lambda_n)\,T_{3,n}(\lambda_n) - T_{1,n}(\lambda_n)T_{4,n}(\lambda_n)} \quad (34)$$

Equations (33) and (34) were introduced in Eq. (25) resulting:

$$\psi_L(\xi,t_d) = \sum_{n=0}^{\infty}\frac{\left\{\sin\varphi_n(\lambda_n)\exp\frac{1}{2}\left[T_{2,n}(\lambda_n)\cos\varphi_n(\lambda_n)\xi - T_{1,n}(\lambda_n)\right.\right.}{T_{2,n}(\lambda_n)T_{3,n}(\lambda_n) - T_{1,n}(\lambda_n)T_{4,n}(\lambda_n)} \sin\varphi_n(\lambda_n)\xi\Big] + \left\{[1-\cos\varphi_n(\lambda_n)]\exp\frac{1}{2}\left[T_{3,n}(\lambda_n)\sin\varphi_n(\lambda_n)\xi\right.\right. - T_{4,n}(\lambda_n)\cos\varphi_n(\lambda_n)\xi\Big]\xi\Big\}\Big\} e^{-\lambda_n^2 t_d} \quad (35)$$

For $\xi = 1$ it is possible to obtain the response at the outlet of the fixed bed by:

$$\psi_L(t_d) = \int_{\xi=0}^{\xi=1} \psi_L(\xi,\tau)\,\delta(\xi-1)\,d\xi \quad (36)$$

hence,

$$\psi_L(t_d) = \sum_{n=0}^{\infty} \frac{1.6\left\{\left[T_{2,n}(\lambda_n) - T_{3,n}(\lambda_n)\sin\varphi_n(\lambda_n)\cos\varphi_n(\lambda_n)\right]\right.}{T_{2,n}(\lambda_n)\,T_{3,n}(\lambda_n) - T_{1,n}(\lambda_n)T_{4,n}(\lambda_n)} + T_{4,n}(\lambda_n)\cos\varphi_n(\lambda_n)\left[\cos\varphi_n(\lambda_n) - 1\right] + \sin\varphi_n(\lambda_n) \quad (37)$$
$$\left.\left[T_{3,n}(\lambda_n) - T_{1,n}(\lambda_n)\sin\varphi_n(\lambda_n)\right]\right\} e^{-\lambda_n^2 t_d}$$

Materials and Methods

The experiments were realized in a three-phase trickle bed reactor, which consists of a fixed bed with a height of 0.22 m and an inner diameter of 0.030 m with catalytic particles contacted by a cocurrent gas-liquid downward flow carrying the liquid tracer in the liquid phase. The experiments were performed at conditions where the superficial velocities of the gas and liquid phases were maintained at such a level to guarantee a low interaction regime with V_{SL} in the range of 1.0 x 10^{-4} m s^{-1} to 3.0 x 10^{-3} m s^{-1} and V_{SG} in the range of 2.0 x 10^{-2} m s^{-1} to 4.5 x 10^{-1} m s^{-1} in pilot plant trickle bed reactors (Ramachandran and Chaudhari, 1983).

Continuous analysis of the KCl tracer, at a concentration of 0.05M, were made using HPLC/UV-CG 480C at the outlet of the fixed bed. The results were expressed in term of the tracer concentrations versus time.

The methodologies applied to evaluate the axial dispersion, liquid-solid mass transfer effect and partial wetting efficiency for the (N_2/H_2O-KCl/activated carbon) system were:

- comparison of the experimental results with Eq. (37), developed for the system;
- evaluation of the model parameters D_{ax}, k_{LS} and F_M; considered as initial estimates values obtained from correlations in Table (2);
- optimization of the model parameters by comparing between the experimental and calculated data by Eq. (37).

The initial values of D_{ax}, k_{LS} and F_M were determined by the empirical correlations as to Table (2).

To calculate the concentrations within the mathematical model, for the system N_2/H_2O - KCl / activated carbon, various parameters have been necessary. These parameters are presented in Table 3.

Table 2. Correlations for the obtainment of the D_{ax}, k_{LS} and F_M, the initial values.

Correlations	References
$D_{ax} = 0.55\,(Re_L)^{0.61}$ (38)	Lange et al. (1999)
$k_{LS} = 2.514\dfrac{\left[1-\left(h_{d,L}/\varepsilon_{ex}\right)\right]D_L}{a_{LS}\,d_p^2}(R_L)^{0.73}(R_G)^{0.2}(Sc_L)^{0.5}\left(\dfrac{d_p}{d_r}\right)^{0.2}$ (39)	Fukushima and Kusaka, (1977)
$F_M = 3.40\,(Re_L)^{0.22}(Re_G)^{-0.08}(Ga_L)^{-0.51}$ (40)	Burghardt et al. (1990)

Table 3. Summary of intervals of operating conditions for the particle-fluid (Colombo et al., 1976 and Silva et al., 2003).

Category	Properties	Numerical Values
Operating conditions	Pressure (P), atm	1.01
	Temperature (T), K	298.00
	Superficial velocity of the liquid phase (V_{SL}) x 10^3, m s^{-1}	6.01 - 0.79
	Superficial velocity of the gas phase (V_{SG}) x 10^2, m s^{-1}	2.50
	Standard acceleration of gravity (g), m s^{-2}	9.81
Packing and bed properties	Total bed height (L) x 10^2, m	0.22
	Bed porosity (ε_p)	0.59
	External porosity (ε_{ex})	0.39
	Effective liquid-solid mass transfer area per unit column volume (a_{LS}) x 10^{-2}, m^{-1}	3.97
	Diameter of the catalyst particle (d_p) x 10^4, m	3.90
	Diameter of the reactor (d_r) x 10^2, m	3.00
	Density of the particle (ρ_p) x 10^{-3}, kg m^{-3}	2.56
	reaction rate constant (k_r) x 10^{-3}, kgmol kg^{-1} s^{-1}	6.33
Liquid properties	Density of the liquid phase (ρ_l) x 10^{-3}, kg m^{-3}	1.01
	Liquid molecular diffusivity (D_L) x 10^7, m^2 s^{-1}	6.89
	Viscosity of the liquid phase (μ_l) x 10^{-4}, kg m^{-1} s^{-1}	8.96
	Surface tension (σ_l) x 10^2, kg s^{-2}	7.31
	Dynamic liquid holdup ($h_{d,l}$)x10^1	4.91
Gas properties	Density of the gaseous phase (ρ_g) x 10^1, kg m^{-3}	6.63
	Viscosity of the gaseous phase (μ_g) x 10^5, kg m^{-1} s^{-1}	1.23

Results and Discussion

Experiments were performed at constant superficial velocity of the gas phase V_{SG} = 2.50 x 10^{-2} m s^{-1} and the liquid phase varying in the range of V_{SL} = (6.01 x 10^{-3} to 7.90 x 10^{-4}) m s^{-1}.

The axial dispersion coefficient, liquid-solid mass transfer coefficient and partial wetting efficiency were determined simultaneously by comparing between the experimental and theoretical data, obtained at the outlet of the fixed bed, subject to the minimization of the objective function (F), given by:

$$F(D_{ax}, k_{LS}, F_M) = \sum_{k=1}^{N} \left\{ [\psi_L(t_d)]_k^{Exp} - [\psi_L(t_d)]_k^{Calc} \right\}^2 \quad (41)$$

The numerical procedure to optimize these parameters involved an optimization subroutine (Box, 1965). The optimized values of the three parameters, for different liquid phase flows, are reported below in Table 4.

Table 4. Optimized values of the axial dispersion, liquid-solid mass transfer and wetting factor at V_{SG} = 2.50 x 10^{-2} m s^{-1}.

Superficial velocity of the liquid phase	Optimized values			Objective function
V_{SL} x 10^3 m s^{-1}	D_{ax} x 10^7 m^2 s^{-1}	k_{LS} x 10^6 m s^{-1}	F_M	F x 10^3
6.01	9.61	7.06	0.57	1.26
5.67	9.21	6.81	0.54	1.24
5.31	8.32	6.67	0.51	1.16
4.95	7.47	6.32	0.47	1.15
4.59	6.77	5.96	0.46	1.12
4.24	5.59	5.78	0.45	1.10
3.89	5.09	5.43	0.43	1.08
3.54	4.47	5.17	0.42	1.07
3.18	3.79	4.97	0.39	1.05
2.83	3.21	4.49	0.37	1.03
2.48	2.87	4.03	0.33	1.01
2.12	2.37	3.67	0.32	0.95
1.78	2.17	2.79	0.27	0.86
1.41	2.12	2.41	0.24	0.78
1.06	2.08	2.09	0.22	0.62
0.79	2.01	1.87	0.21	0.47

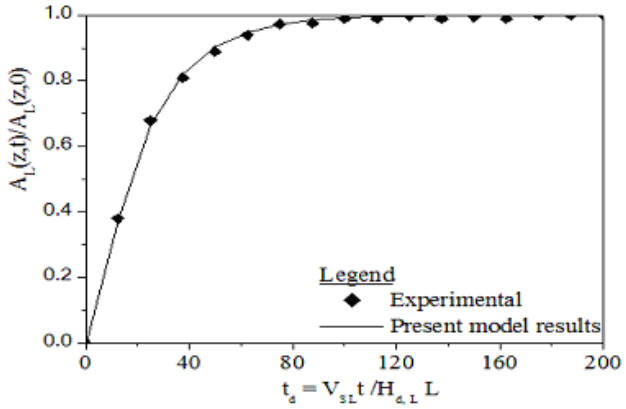

Figure 1. Validation of the tracer concentration at the outlet of the N_2/H_2O-KCl/activated carbon: ♦ results in gas and liquid superficial velocities V_{SG} = 2.50 x 10^{-2}m s^{-1} and V_{SL} = 2.48 x 10^{-3}m s^{-1}; — results in parameters D_{ax} = 2.87 x 10^{-7} m^2s^{-1}, k_{LS} = 4.03 x 10^{-6} m s^{-1}, F_M = 0.33 and F = 1.01 x 10^{-3}.

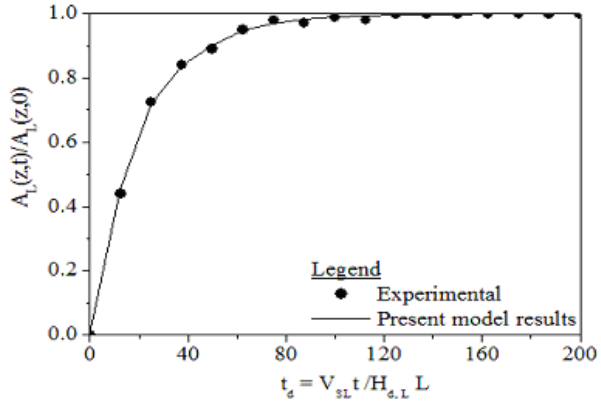

Figure 2. Validation of the tracer concentration at the outlet of the N_2/H_2O-KCl / activated carbon: ● results in gas and liquid superficial velocities V_{SG} = 2.50 x 10^{-2}m s^{-1} and V_{SL} = 2.83 x 10^{-3}m s^{-1}; — results in parameters D_{ax} = 3.21 x 10^{-7} m^2s^{-1}, k_{LS} = 4.49 x 10^{-6} m s^{-1}, F_M = 0.37 and F = 1.03 x 10^{-3}.

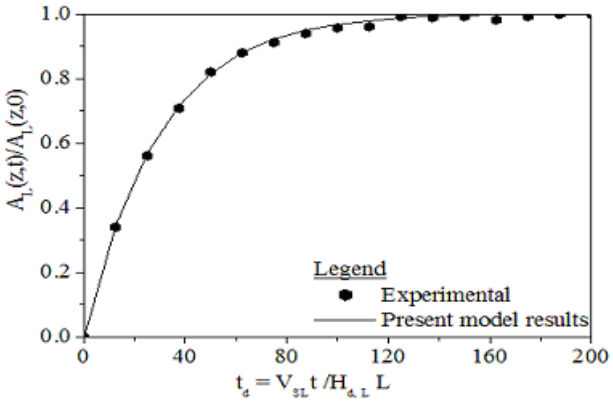

Figure 3. Validation of the tracer concentration at the outlet of the N_2/H_2O-KCl / activated carbon: ● results in gas and liquid superficial velocities V_{SG} = 2.50 x 10^{-2}m s^{-1} and V_{SL} = 5.31 x 10^{-3}m s^{-1}; — results in parameters D_{ax} = 8.32 x 10^{-7} m^2s^{-1}, k_{LS} = 6.67 x 10^{-6} m s^{-1}, F_M = 0.51 and F = 1.16 x 10^{-3}.

A model validation process was established by comparing the theoretical results obtained with the values of the optimized parameters and the experimental data for three tests. The results presented in Figs. 1 to 3 confirm this model.

The axial dispersion coefficient, liquid-solid mass transfer coefficient and the wetting efficiency are influenced by changes in the liquid flow. The behavior of D_{ax}, k_{LS} and F_M can be described by the empirical correlations, Eqs. (42), (43) and (44). They are restricted to following operation ranges: d_p = 3.90 x10^{-4}, 1496 ≤ Re_L ≤ 178, 0.89 ≤ Sc_L ≤ 4.18 and 0.21 ≤ F_M ≤ 0.57.

$$D_{ax} = 37.04(Re_L)^{-0.18}(F_M)^{2.07}, \; R = 0.9982 \quad (42)$$

$$k_{LS} = 2.87(Re_L)^{0.53}(Sc_L)^{0.23}, \; R = 0.9979 \quad (43)$$

$$F_M = 0.47(Re_L)^{0.39}, \; R = 0.9981 \quad (44)$$

Figures (4), (5) and (6) present parity plots of the obtained results. The parameters D_{ax}, k_{LS} and F_M were fitted by the least-squares method via empirical correlations presented in Eqs. (42), (43) and (44).

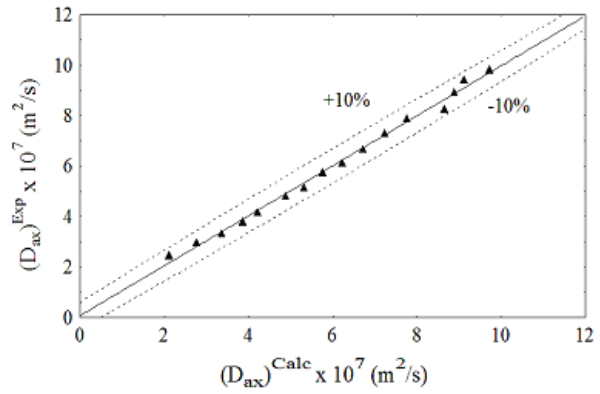

Figure 4. $(D_{ax})^{Exp}$ vs. $(D_{ax})^{Calc}$ for the system N_2/H_2O- KCl / activated carbon in low interaction. V_{SL} = (6.01 x 10^{-3} to 7.90 x 10^{-4}) m s^{-1} and V_{SG} = 2.50 x 10^{-2} m s^{-1}.

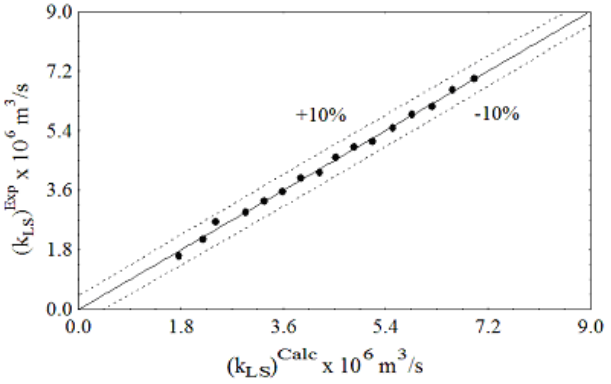

Figure 5. $(k_{LS})^{Exp}$ vs. $(k_{LS})^{Calc}$ for the system N_2/H_2O- KCl / activated carbon in low interaction. V_{SL} = (6.01 x 10^{-3} to 7.90 x 10^{-4}) m s^{-1} and V_{SG} = 2.50 x 10^{-2} m s^{-1}.

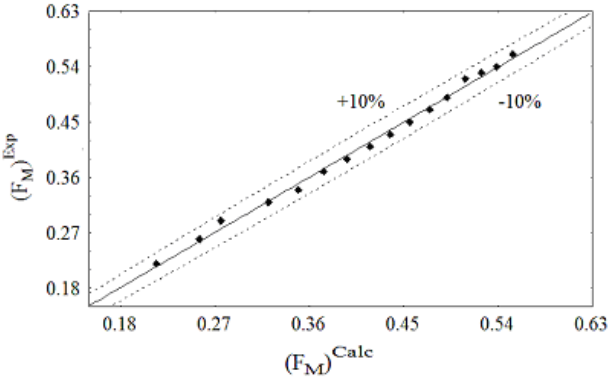

Figure 6. $(F_M)^{Exp}$ vs. $(F_M)^{Calc}$ for the system N_2/H_2O- KCl / activated carbon in low interaction. V_{SL} = (6.01 x 10^{-3} to 7.90 x 10^{-4}) m s^{-1} and V_{SG} = 2.50 x 10^{-2} m s^{-1}.

Conclusion

Based on the experimental and modelling studies of the liquid phase in a low interaction system, the following results were obtained: (i) the estimation of the parameters D_{ax}, k_{LS} and F_M, (ii) the validation of the model and (iii) the analysis of the behavior of the axial dispersion coefficient, liquid-solid mass transfer coefficient and wetting efficiency by new forms of empirical correlations, Eqs. (42), (43) and (44). The final values of the parameters were obtained with values of the objective function, F = 1.26 x 10^{-3} to 4.70 x 10^{-4}. Thus, the range of the optimized values of the parameters by fitting between the theoretical and experimental response was given as: D_{ax} = 9.61 x 10^{-7} m^2 s^{-1} to 2.01 x 10^{-7} m^2 s^{-1}, k_{LS} = 7.06 x 10^{-6} m s^{-1} to 1.87 x 10^{-6} m s^{-1} and F_M = 0.57 to 0.21.

Acknowledgements

The authors would like to thank CNPq (Conselho Nacional de Desenvolvimento Tecnológico) for financial support (process 483541/07-9).

References

Al-Dahhan, M.H., Larachi, F., Dudukovic, M.P., Laurent, A., 1997, "High-pressure trickle bed reactors: a review", *Industrial Engineering Chemical Research*, Vol. 36, pp. 3292-3314.

Augier, F., Koudil, A., Muszynski, L., Yanouri, Q., 2010, "Numerical approach to predict wetting and catalyst efficiencies inside trickle bed reactors", *Chemical Engineering Science*, Vol. 65, pp. 255-260.

Ayude, A., Cechini, J., Cassanello, M., Martínez, O., Haure, P., 2008, "Trickle bed reactors: effect of liquid flow modulation on catalytic activity", *Chemical Engineering Science*, Vol. 63, pp. 4969-4973.

Box, P., 1965, "A new method of constrained optimization and a comparison with other method", *Computer Journal*, Vol. 8, pp. 42-52.

Burghardt A., Bartelmus G., Jaroszynski M., Kolodziej A., 1995, "Hydrodynamics and mass transfer in a three-phase fixed bed reactor with concurrent gas-liquid downflow", *Chemical Engineering and Processing*, Vol. 28, pp. 83-99.

Burghardt A., Kolodziej, A.S., Jaroszynski M., 1990, "Experimental studies of liquid-solid wetting efficiency in trickle-bed concurrent reactors", *Chemical Engineering Journal*, Vol. 28, pp. 35-49.

Colombo A.J., Baldi G., Sicardi S., 1976, "Solid-liquid contacting effectiveness in trickle-bed reactors", *Chemical Engineering Science*, Vol. 31, pp. 1101-1108.

Dudukovic, M.P., Larachi, F., Mills, P.L., 1999, "Multiphase reactors-revisited", *Chemical Engineering Science*, Vol. 54, pp. 1975-1995.

Dudukovic M.P., 1982, "Analytical solution for the transient response in a diffusion cell of the wickle- kallenbach type", *Chemical Engineering Science*, Vol. 37, pp. 153-158.

Feike J. L., Toride N., 1998, "Analytical solutions for solute transport with binary and ternary exchange", *Soil Sci. Soc. Am. J*, Vol. 56, pp. 855-864.

Fukushima, S., Kusaka, K., 1977, "Interfacial area boundary of hydrodynamic flow region in packed column with concurrent downward flow", *Journal of Chemical Engineering of Japan*, Vol. 10, No. 6, pp. 461-467.

Iliuta, I, Bildea, S.C., Iliuta, M.C., Larachi, F., 2002, "Analysis of trickle-bed and packed bubble column bioreactors for combined carbon oxidation and nitrification", *Brazilian Journal of Chemical Engineering*, Vol. 19, pp. 69-87.

Lange, R., Gutsche, R., Hanika, J., 1999, "Forced periodic operation of a trickle-bed reactor", *Chemical Engineering Science*, Vol. 54, pp. 2569-2573.

Latifi, M.A., Naderifar, A., Midoux, N., 1997, "Experimental investigation of the liquid-solid mass transfer at the wall of trickle-bed – Influence of Schmidt Number", *Chemical Engineering Science*, Vol. 52, pp. 4005-4011.

Liu, G., Zhang, X., Wang, L., Zhang, S., Mi, Z., 2008, "Unsteady-state operation of trickle-bed reactor for dicyclopentadiene hydrogenation", *Chemical Engineering Science*, Vol. 36, pp. 4991-5001.

Ramachandran P.A., Chaudhari, R.B., 1983, "Three phase catalytic reactors", *Gordan and Breach Science Publishers*, New York, U.S.A., Chap. 7, pp. 200-255.

Rodrigo J.G., Rosa, L., Quinta-Ferreira, M., 2009, "Turbulence modelling of multiphase flow in high-pressure trickle reactor", *Chemical Engineering Science*, Vol. 64, pp. 1806-1819.

Satterfield, C.N., Van Eck, M.W., Bliss, G.S., 1978, "Liquid - Solid mass transfer in packed beds with downflow cocurrent gas-liquid flow", *Aiche J.*, Vol. 24, pp. 709-721.

Silva, J.D., Lima, F.R.A.; Abreu, C.A.M.; Knoechelmann, A., 2003, "Experimental analysis and evaluation of the mass transfer process in a trickle bed regime", *Brazilian Journal of Chemical Engineering*, Vol. 20, No. 4, pp. 375-390.